JOURNAL OF APPLIED POLYMER SCIENCE VOL. 20, 1339–1353 (1976)

A Light-Scattering and Membrane Formation Study on Concentrated Cellulose Acetate Solutions

B. KUNST, *Institute of Physical Chemistry, University of Zagreb, 41001 Zagreb,* Đ. ŠKEVIN, *Pliva, Pharmaceutical and Chemical Works, Zagreb,* Gj. DEŽELIĆ, *Andrija Štampar School of Public Health, Faculty of Medicine, University of Zagreb,* J. J. PETRES,* *Institute Rugjer Bošković, Zagreb, Yugoslavia*

Synopsis

An improved explanation of the mechanism of the porous membrane formation with asymmetric structure has been proposed. It emerged from the correlation of the results obtained by the light-scattering measurements of the ternary membrane casting solutions and by the reverse osmosis and ultrafiltration testing of the asymmetric membranes prepared from these solutions. The results of anisotropic light-scattering measurements indicated the extent of supermolecular structurization of the casting solution which affected the porous structure formation in the membrane surface region. The variation of the casting solution composition and, particularly, the role of the CA/F ratio, the formamide content, and their influence on the asymmetric membrane properties were investigated and explained using the improved concept of the membrane-making mechanism.

INTRODUCTION

Loeb-Sourirajan's discovery[1] of the porous asymmetric membrane fabrication method opened a new field in separation technology: pressure-driven membrane separation and concentration processes. A substantial progress has since been accomplished in the membrane science and in the application of the membrane separation processes (reverse osmosis and ultrafiltration) in industry. Notwithstanding appreciable improvements in the membrane performance, developments of a number of new membrane materials, and the utilization of new fabrication methods, the initially introduced cellulose acetate porous asymmetric film is still, in an improved form, the most often used membrane in actual separation processes. Cellulose acetate has also been the most convenient model polymer for the membrane studies which aim at producing better, more productive or more selective membranes and/or shedding more light on the process of the asymmetric membrane formation.

The first coherent picture of the mechanism of the porous asymmetric membrane formation was proposed by Kesting.[2,3] It has further been improved by the solution structure–evaporation rate concept[4–10] and by the in-

* Present address: Institute of Immunology, Zagreb, Yugoslavia.

vestigation of the dynamics of the membrane formation process.[11-16] All the studies mentioned have contributed to a better understanding of the relevant processes taking place during the membrane formation, and some of them have even directly led to membranes of better performance. However, there are still uncertainties in the explanation of the sequence of events occurring from the casting of the polymer solution layer to the finally formed porous asymmetric membrane. One of such unresolved problems is the effect of the casting solution structure on the phase inversion process in the cast solution layer. There is a general agreement[2,5,6,13,17,18] that the morphology of a membrane surface layer originates in the structure of the polymer solution. There have also been attempts[5] to define the extent of solution structurization, but as yet neither the effective means of expressing the solution structure nor a satisfactory correlation of this structure to the membrane properties has been elaborated.

The aim of this study is to elucidate the early stage of the membrane formation process by investigating the correlation between the extent of the casting solution structurization and the properties of the resultant membrane. A model system cellulose acetate (CA)–acetone–formamide has been studied by the light-scattering measurement, a method applied in the attempt to assess the extent of solution structurization. The casting solution compositions have been chosen to give relatively big-pored membranes, such as those used in ultrafiltration processes.

EXPERIMENTAL

Materials and Solutions

Eastman cellulose acetate (E-398-3) and reagent-grade acetone and formamide Merck, Darmstadt, W. Germany, were employed for both the solution preparations for light-scattering measurements and for the casting of membranes. A reagent-grade sodium chloride and globular proteins, such as glucagon, insulin, trypsin, pepsin, ovalbumin, hemoglobin, gamma globulin, etc., were used as test substances for the determination of membrane porosities.

The binary CA–acetone and ternary CA–acetone–formamide solutions of various compositions (Table I) were prepared.

Light-Scattering Measurements

Light-scattering measurements were performed by using a Brice-Phoenix Model 2000-DMS light-scattering photometer, manufactured by Phoenix Precision Instrument Co., Philadelphia, Pa., U.S.A. A Philips SP-500-W water-cooled superpressure mercury lamp was used as the light source. All details of the experimental setup and instrument calibration were the same as those described previously.[19] The measurements of the solutions were performed in Zimm-type conical cells situated in the center of a cylindrical cell painted black at the outer back surface. The conical cell was immersed in the solvent of the same composition as was used for polymer dissolution. Absolute Rayleigh ratios were determined by the standard scatterer method.[20] Benzene served as the primary and a cube of Perspex, as the secondary

TABLE I
Compositions of CA Solutions

Type	Content, wt-%			CA/F ratio
	CA	Acetone	Formamide	
1.1	10	90	—	
1.2	12.5	87.5	—	
1.3	15	85	—	
1.4	17	83	—	
1.5	20	80	—	
1.6	25	75	—	
2.1	10	55	35	0.286
2.2	12.5	52.5	35	0.357
2.3	15	50	35	0.429
2.4	17	48	35	0.486
2.5	20	45	35	0.571
2.6	25	40	35	0.714
3.1	10	45	45	0.222
3.2	12.5	42.5	45	0.278
3.3	15	40	45	0.334
3.4	17	38	45	0.378
3.5	20	35	45	0.445
4.1	17	53	30	0.568
4.2	17	48	35	0.486
4.3	17	43	40	0.425
4.4	17	38	45	0.378
4.5	17	33	50	0.340

standard. The clarification of all solutions was performed by centrifugation at 24,000 rcf for 2 hr. The measurements were performed at the wavelength of incident light $\lambda_0 = 546$ nm at room temperature.

Membrane Preparation and Testing

Porous asymmetric membranes were cast by the standard procedure[4] from all the solutions listed in Table I. The film-casting conditions used were as follows: temperature of the casting solution, 0–5°C; temperature of the casting atmosphere, 10–15°C; relative humidity of the casting atmosphere, 65%; evaporation period, 2–5 sec; gelation medium, ice-cold water; gelation period, at least 1 hr. The temperature of the glass plate on which the film was cast was the same as the temperature of the casting solution.

The membranes obtained by the casting procedure were tested in both the ultrafiltration static cell and the reverse osmosis flow cells. The first kind of the experiment was performed in a Millipore laboratory cell, type XX 4209050, provided with an agitator. Each membrane was first subjected to a pure-water pressure of 6 atm for 1 hr to stabilize its porous structure. The ultrafiltration experiment was started 2 hr after the pressurization was completed and the pressure released. It was done at 5 atm, and the results of the membrane water flux and its protein retention value (PRV) were collected. The PRV is the value of the molecular weight of a globular protein which was completely retained on the membrane. The absence of protein in the ultraf-

iltrate was checked by the negative precipitation test with 20% trichloroacetic acid.

Determinations of the membrane shrinkage profiles were carried out in the reverse osmosis flow cells. Before the reverse osmosis test, membranes were thermally shrunk at different temperatures to give different levels of solute separations at preset operating conditions. After thermal treatment, all the membranes were subjected to a pure-water pressure of 10.5 atm in the flow cells for 1 hr. The reverse osmosis experiment of the short-run type was performed at the laboratory temperature, using the aqueous feed solution containing 200 ppm NaCl and a feed rate of 450 cc/min at the operating pressure of 7 atm. The solute separation f, defined as

$$f = \frac{\text{ppm}_{\text{NaCl}} \text{ in feed} - \text{ppm}_{\text{NaCl}} \text{ in product}}{\text{ppm}_{\text{NaCl}} \text{ in feed}}$$

was determined in each experiment. The solute concentrations in feed and product solutions were determined by specific resistance measurements using a conductivity cell.

RESULTS

Values of both the concentration and anisotropic Rayleigh ratios, R_c and R_{anis}, respectively, were evaluted from directly measured total Rayleigh ratio, R_u, values and the partial Rayleigh ratio, H_v, values. The procedure for calculating R_c and R_{anis} is described in the following text.

From the general light-scattering theory[19,20] it follows that R_{anis} can be determined directly from measured H_v values:

$$R_{anis}(\vartheta) = (13 + \cos^2\vartheta)H_v(\vartheta)/6. \tag{1}$$

Since

$$R_u(\vartheta) = R_{is}(\vartheta) + R_{anis}(\vartheta) \tag{2}$$

it follows that

$$R_{is}(\vartheta) = R_u(\vartheta) - (13 + \cos^2\vartheta)H_v(\vartheta)/6. \tag{3}$$

$R_{is}(\vartheta)$ is related to the isotropic molecular scattering factor F_{is}, a quantity depending only on thermodynamic parameters and not depending on the scattering angle ϑ, by the expression

$$R_{is}(\vartheta) = (\pi^2/2\lambda_0^4)(1 + \cos^2\vartheta)F_{is}. \tag{4}$$

It is customary to express the isotropic Rayleigh ratio R_{is} as a sum of the density, concentration, and cross-term Rayleigh ratios R_d, R_c, and $R\#$, respectively. Since these terms do not depend on the scattering angle, only $R_{is}(90)$ or the normalized values $R_{is}(\vartheta)/(1 + \cos^2\vartheta)$ should be used in the evaluation of R_c. For scatterers failing to meet the conditions of the Rayleigh scattering (the size of particles or molecules small in comparison with the wavelength), the Rayleigh-Debye approach should be used, and the form factor $P(\vartheta)$ should be taken into account; thus, the evaluation of R_c should be performed with $R_{is}(\vartheta)/(1 + \cos^2\vartheta)P(\vartheta)$ values. Since it was beyond the scope of this study to determine the form factors owing to yet unknown behavior of these functions in concentrated polymer solutions, it suffices to take

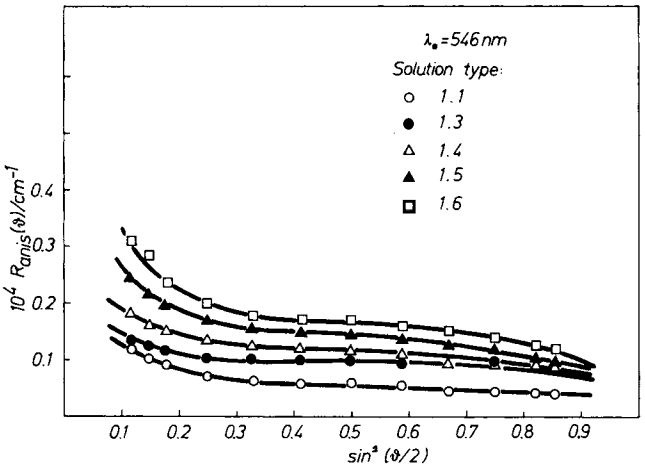

Fig. 1. Angular dependence of anisotropic Rayleigh ratio R_{anis} for CA solutions in acetone.

$P(\vartheta)$ as constant and observe only values for $\vartheta = 90°$, indicating variations in the molecular and/or aggregate size. The following expression for R_c can be used:

$$R_c = R_{is}(90) - R_d - R^{\#}. \tag{5}$$

In the case of polymer solutions, the $R\#$ term can be neglected, as was shown earlier[19]; it should be taken into account only for solutions with small R_c values, and this is the case with solutes having a molecular weight comparable to that of the solvent. The term R_d could be determined from the physical constants of the solution only, but unfortunately, these data are not available yet. In this situation, and taking into consideration the fact that

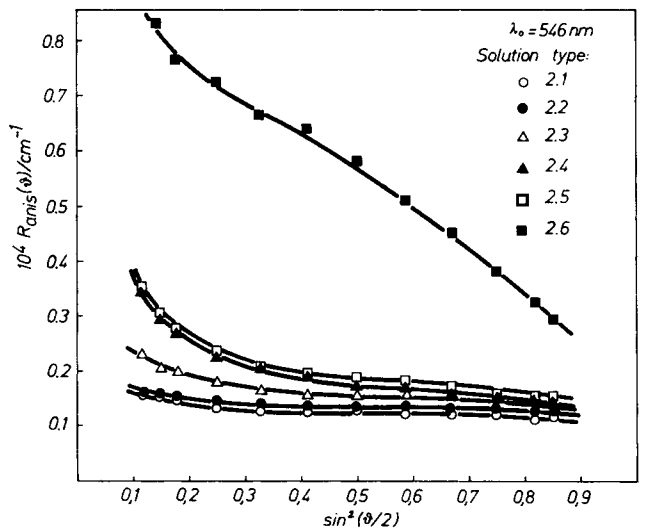

Fig. 2. Angular dependence of anisotropic Rayleigh ratio R_{anis} for typical CA–acetone–formamide system.

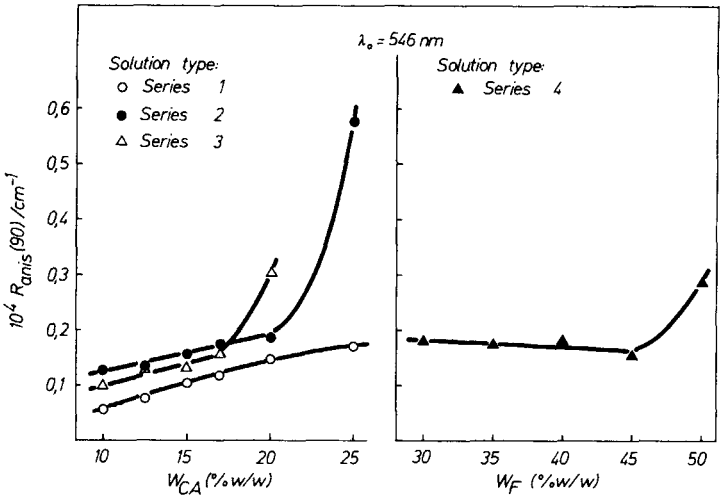

Fig. 3. Anisotropic Rayleigh ratios $R_{anis}(90)$ for all the CA solutions investigated as a function of CA and formamide content.

the R_d values lie in the range of several percentages of R_{is} values for polymer solutions, the approximation

$$R_d = R_{is,\,\text{solvent}}(90) \tag{6}$$

was found justifiable.

In Figure 1, the angular dependence of $R_{anis}(\vartheta)$ is shown for cellulose acetate solutions in acetone. Only a small increase of anisotropic scattering with an increasing CA concentration is noted. The values are almost constant with ϑ, the small increase at lower ϑ can be primarily ascribed to the presence of dust and mechanical impurities, which could not be fully eliminated by the

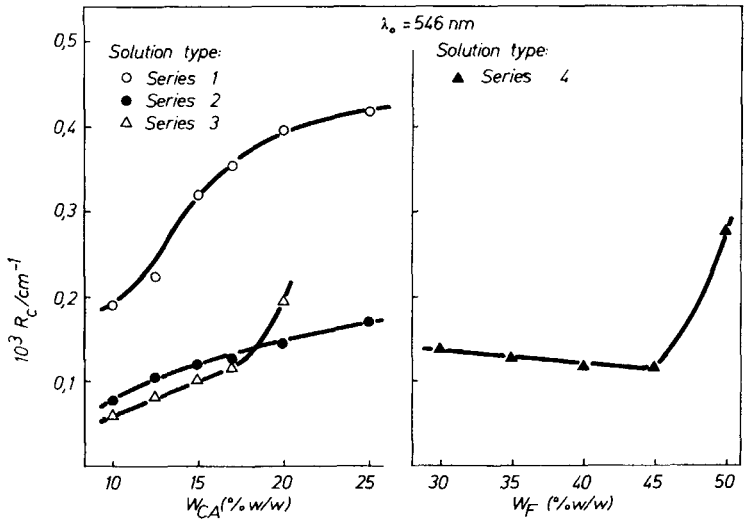

Fig. 4. Concentration Rayleigh ratios R_c for all the CA solutions investigated as a function of CA and formamide content.

TABLE II
Results of Ultrafiltration Experiments

Membrane type[a]	CA/F ratio	Retention limit mol. weight[b]	Normalized water flux, ml/hr atm cm²
1.1	—	—	—
1.2	—	—	—
1.3	—	—	—
1.4	—	—	—
1.5	—	—	—
1.6	—	—	—
2.1	0.286	80,000	36.4
2.2	0.357	70,000	13.4
2.3	0.429	40,000	9.1
2.4	0.486	30,000	8.0
2.5	0.571	5,000	4.1
2.6	0.714	1,000	3.0
3.1	0.222	100,000	46.0
3.2	0.278	90,000	24.8
3.3	0.334	60,000	17.9
3.4	0.378	40,000	14.8
3.5	0.445	25,000	5.7
4.1	0.568	1,000	1.7
4.2	0.486	30,000	8.0
4.3	0.425	40,000	11.6
4.4	0.378	40,000	14.8
4.5	0.340	40,000	9.1

[a] Membranes have the same designations as the casting solutions they are made from (see Table I).

[b] Approximate values based on the retention of test substances.

clarification procedure, and to some extent to secondary scattering. In contrast to this picture, corresponding graphs for CA–acetone–formamide solutions show a sharp increase in $R_{anis}(\vartheta)$ values at a certain higher CA or formamide content. Typical curves of such a type are shown in Figure 2 for the solutions of series 2.

Figures 3a and 3b give the anisotropic scattering data, $R_{anis}(90)$, for all the solutions measured. The diagrams presented show that R_{anis} values for the ternary CA solutions are generally higher than those for the binary ones. Two features of the results presented seem to be particularly important: (i) a systematic gradual increase of $R_{anis}(90)$ values in a wide range of CA concentrations in solutions of series 1, 2, and 3 as contrasted with the constancy or even a slight decrease of $R_{anis}(90)$ values obtained by the increase of the formamide content in solutions of series 4; and (ii) the exceptionally high R_{anis} values of the solutions having the highest concentration of CA (in series 2 and 3 with the constant formamide content) and the highest concentration of formamide (in series 4).

The R_c values for the investigated solutions are shown in Figures 4a and 4b. They are in the order of magnitude higher than the corresponding R_{anis} values. The R_c-versus-w_{CA} curve of the binary CA–acetone system smoothly increases with the CA concentration and is located at markedly higher values than the curves for ternary CA–acetone–formamide systems. The curves for

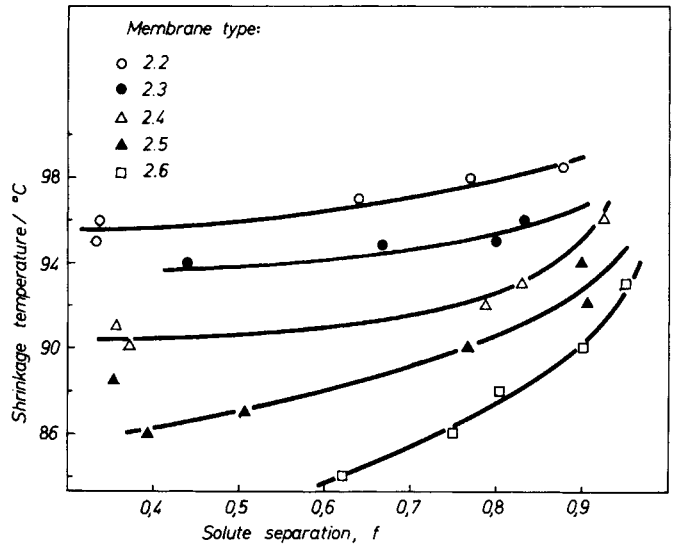

Fig. 5. Shrinkage temperature profiles for the membranes of series 2. Conditions of reverse osmosis test: operating pressure, 7 atm; testing solution, 200 ppm sodium chloride.

the solutions of series 3 and 4 show a rather sharp increase of R_c values at higher CA and/or formamide concentrations.

The results of membrane testing are divided into two parts, the ultrafiltration tests and the shrinkage temperature profile determinations. The results of the ultrafiltration experiments are given in Table II. Besides the CA/F ratios of the solutions used to cast the membranes, the approximate protein retention values and the values of normalized water fluxes through the membranes are presented. The membranes cast from the binary CA solutions in acetone were not permeable at all. For those made from the ternary solu-

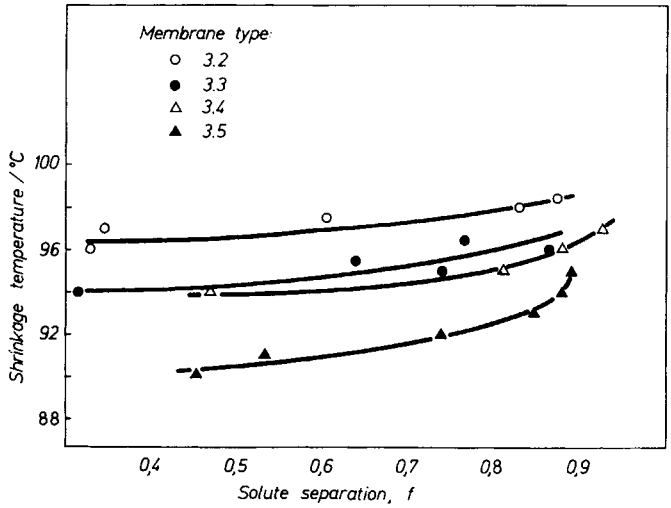

Fig. 6. Shrinkage temperature profiles for the membranes of series 3. Conditions of reverse osmosis test: operating pressure, 7 atm; testing solution, 200 ppm sodium chloride.

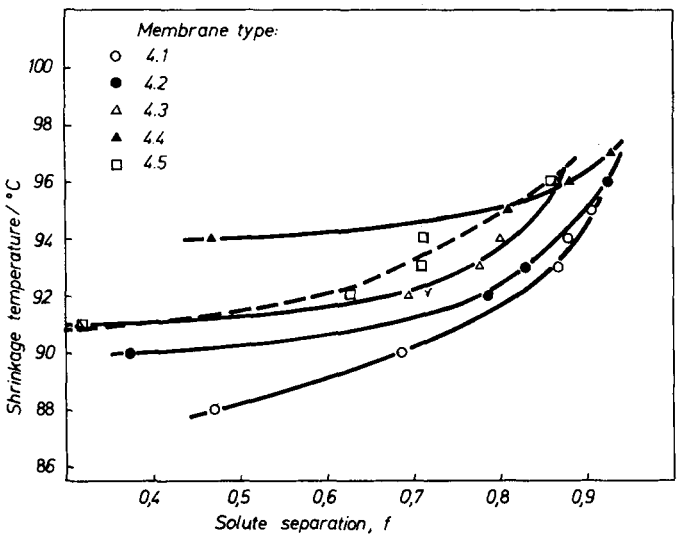

Fig. 7. Shrinkage temperature profiles for the membranes of series 4. Conditions of reverse osmosis test: operating pressure, 7 atm; testing solution, 200 ppm sodium chloride.

tions, both values (PRV and normalized water flux) vary with the change in the casting solution composition, i.e., with its CA/F ratio. An increase in the CA/F ratio brings about a regular drop in the PRV as well as in the normalized water fluxes for membranes of series 2 and 3. A similar tendency, but with some minor exceptions, is valid also for the membranes of series 4.

The membranes investigated were also shrunk at different temperatures and subsequently tested in the reverse osmosis experiment. By this procedure, shrinkage temperature profiles, i.e., shrinkage temperature versus sodium chloride separation dependences, were obtained (Figs. 5–7). Such diagrams provide useful information on the relative pore size on the membrane surface in the as-cast condition. A higher shrinkage temperature for a given level of solute separation would indicate the presence of relatively bigger average pores on the membrane surface. In the case of membranes of series 2 (Fig. 5), those marked 2.2 can be considered to have relatively the biggest pores and, consequently, the films of type 2.6 to have the smallest ones. Similar conclusions can be made for the membranes of series 3 and 4 (Figs. 6 and 7).

DISCUSSION

In a structurally complex system, like a ternary solution containing polymer at a high concentration and solvents with different interaction constants, it is not easy to explicitly explain light-scattering data, since a rigorous theory of light scattering in concentrated polymer solutions is not available. Discussion on the light-scattering results obtained with such systems is therefore bound to be merely a qualitative one.

From the theory of light scattering, it is known that the concentration Rayleigh ratio R_c depends mainly on thermodynamic quantities and on the particle or molecule size, including molecular interactions, whereas the anisotropic

Rayleigh ratio R_{anis} is a function of the optical anisotropy of molecules or molecular aggregations, i.e., it detects structural ordering in the system. The extent of structural ordering in the concentrated CA solutions expressed by means of the R_{anis} values measured in this work varies noticeably with compositional changes of the casting solution. The significance of this effect can be fully recognized if the R_{anis} values of different casting solutions are examined in connection with the phase separation conditions in a ternary system CA–acetone–formamide and correlated with the performance of membranes cast from these solutions.

If CA is considered to be a single component (i.e., the polydispersity of the sample is neglected), all the ternary solutions investigated in this work can be represented in a triangular diagram (Fig. 8) by points located closer or farther away from the phase separation boundary determined earlier.[7] The solutions of series 2 and 3 (Table I) gradually approach the phase separation line.

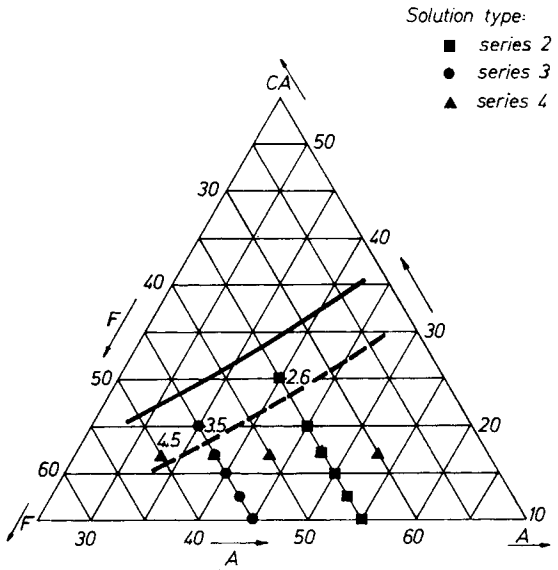

Fig. 8. Locations of the CA solutions investigated in relation to the phase separation conditions.

The CA/F ratio of these solutions steadily increases, followed by a gradual increase of their R_{anis} values (Fig. 3a), i.e., by a progressive increase of supermolecular structurization. On the other hand, a systematic approach to the phase separation line does not necessarily mean an increase in the R_{anis} value, unless such a change is accompanied by an increase of the CA/F ratio. This is the case with the solutions of series 4: their composition points gradually approach the phase separation boundary but their CA/F ratio decreases (Table I), and the R_{anis} values decrease slightly (Fig. 3b), indicating some structural disordering. These considerations lead to a general conclusion that an increase of the CA/F ratio, which brings the solution closer to the phase separation conditions, results in a more extensive supermolecular structurization of the casting solution.

The question arises of how such changes in the casting solution affect the formation of a porous asymmetric membrane. To answer this question, a brief review is needed of the asymmetric membrane formation mechanism as has been described earlier.[2,3,4–7] The membrane formation process begins when a multicomponent polymer (CA) solution, containing a higher or lesser amount of supermolecular aggregates, is cast onto a suitable glass surface. At this moment, the evaporation of the solvent starts, and after a while, the point is reached when the system separates into two phases. During this phase-inversion process, tiny droplets of the dispersed phase (a mostly nonsolvent and swelling agent) appear. They are surrounded by polymer molecules and/or supermolecular aggregates. By continuing desolvation, the droplets grow and approach one another, eventually making contacts in the initial stage of gelation. This is followed by their deforming into polyhedra, a subsequent contraction of polyhedra and the rupturing of their walls, and, finally, the formation of open-celled, porous structure in the membrane surface region.

This mechanism points to the important role of the structure of the casting solution in the early stage of the membrane formation. The precise form and the exact behavior of supermolecular polymer structures in the casting solution before and during the phase inversion process have not as yet been fully visualized. It has been considered[6,7] that larger aggregates exist in the casting solution that is closer to the phase separation conditions and that by using such a casting solution, the formation of effectively bigger pores in the finally produced membrane would be favored.

The findings in this work fail to fit in well with the mechanism described. Although the aforementioned light-scattering results did point to the increase in the casting solution structurization caused by the increased CA/F ratio and the approach toward the phase separation conditions, such a change did not produce effectively bigger pores on the surface of the finally formed membrane. On the contrary, the pore size in the surface layer of membranes from series 2 and 3 dropped, which was shown by the lower limits of protein retention (Table II) and by the shift of the membrane shrinkage profiles toward lower temperature values (Figs. 5 and 6).

In order to explain this discrepancy, i.e., to logically connect the appearance of effectively smaller average pores in the membrane surface region with the observed enlarged ordering in the corresponding casting solutions, we propose here an improved picture of the phase-inversion process. This is based on the notion that the mechanism of the process depends a great deal on the nature of the casting polymer solution. The solutions used for this purpose are, as a rule, highly concentrated (more than 10%), and the polymer itself (usually CA) is specially capable of creating the secondary intermolecular hydrogen bonds. It is, therefore, reasonable to imagine that the supermolecular structurization in such a concentrated solution exists in the form of a long-range dynamic network rather than in the form of independent larger or smaller CA aggregates. Such a type of solution structurization has actually been found in some binary CA systems.[21] If so, the phase-inversion process, i.e., the appearance of dispersed phase droplets would take place within the dynamic polymer network present in the casting solution. The size and number of droplets accommodated in the polymer network would depend on

the dimensions and density of this network and on its resistance toward thermal motion, which randomly breaks and forms the secondary intermolecular bonds. This means that an initially denser and larger CA network in solution would help the creation of smaller and less numerous droplets during the phase-inversion process, producing the surface region ("skin") with smaller average pores in the finally formed membrane. The dispersed phase droplets once formed could move within the dynamic polymer network prior to the completion of a process, but in a restricted fashion and not freely as was assumed in the previous description; in this way, some droplet coalescence and growth could also take place.

Using such a more elaborate picture of the phase inversion process, one can easily explain all the results obtained in this work. The progressively enlarged supermolecular structurization, indicated by the higher R_{anis} values and caused by the increase of the CA/F ratio of the solutions of series 2 and 3, favors the formation and accommodation of progressively smaller and less numerous droplets within the polymer network. As a direct consequence, the membranes having effectively smaller average pores in the surface region, and hence showing better protein retentions, have been prepared. Thus, the proposed picture of the asymmetric membrane formation gives a logical link between the extent of the casting solution structurization and the properties of the resultant membrane. One should have in mind, however, that the extent of ordering in the casting solution is not the only parameter that determines the membrane properties in the as-cast condition. There are other factors in the process of membrane formation, such as the growth of created droplets and their coalescence, but they can also be incorporated into the refined picture of the porous asymmetric membrane formation.

A special role of formamide (the swelling agent) in the casting solution has already been emphasized.[2,3] Our results and the proposed description of the phase-inversion process throw more light on the function of the swelling agent in the process. The typical effect of formamide can be figured out from the comparison of both the light scattering results and the membrane properties.

An increase of the formamide content in the ternary casting solution results in the lower R_{anis} values. This is shown by the location of the curves for solutions of series 2 and 3 in Figure 3a as well as directly by the slight downward trend of the R_{anis}-versus-w_F dependence in Figure 3b. The observed variations point to a diminished structurization in the solutions of a higher formamide content, which may be attributed to the improved solvent power of the acetone–formamide combination toward CA. Such a conclusion is firmly supported by a marked decrease of R_c values for formamide containing systems (Fig. 4a) in relation to the binary CA–acetone mixtures, a result which clearly indicates stronger polymer–solvent interactions in the investigated ternary CA–acetone–formamide systems.

These findings are consistent with Kesting's conclusion[2,3] that formamide increases the solvent power of acetone in the CA solutions. In view of the improved concept of the phase inversion process this result can be explained by the loosening of the supermolecular network and the existence of smaller dynamic units in it if the formamide content in the solution is higher. Such a

role of formamide might be due to its strong tendency of forming intermolecular CA–formamide hydrogen bonds at the expense of the CA–CA intermolecular bonding responsible for the creation of an extensive long-range network in the solution.

The variation of the formamide content and its effect on the casting solution structure must also be reflected in the membrane properties. This is really the case: the PRV's of the series 2 membranes made from the solutions of the lower formamide content are regularly lower (Table II) in comparison with those of the membranes from series 3, indicating the presence of smaller effective pores in the former membrane types. In addition, a systematic increase in the formamide content produced in the series 4 solutions obviously increases the PRV of the membrane. A similar conclusion can be reached from the shrinkage temperature profiles of the membranes from series 2 and 3 (Figs. 5 and 6). The shrinkage temperature profiles of the series 2 films are, as a rule, located at the lower temperatures than those of the series 3 membranes, pointing again to the presence of smaller pores in the series 2 films. Furthermore, a comparison of the shrinkage temperature profiles within the series 4-type membranes shows an upward shift of the curves for membranes made from formamide-richer solutions, which suggests a systematic increase in the effective membrane pore size. All these results consistently confirm the validity of the improved membrane formation concept, which takes into account the structure of the casting solution and its influence on the events occurring later in the process.

The role of formamide seems to change in the solutions approaching the phase separation conditions. This is illustrated by solutions 2.6, 3.5, and 4.5 represented by the points (Fig. 8) located at an approximately equal distance (dotted line) from the phase separation boundary. Their R_{anis} values deviate strongly from the obvious trends (Figs. 3a and 3b). The unexpected increase of the R_{anis} values for the solutions mentioned implies a fast, extensive ordering in the solutions closely approaching the phase separation boundary. As a consequence, there is also an unusual change in the properties of the membranes made from these solutions, which is most clearly seen in the series 4 membranes. The irregular change in the membrane porosities is manifested by the lowering of the shrinkage temperature profile of membranes 4.5 (Fig. 7) as contrasted to the upward trend in the other profiles, and by the constancy of the retention limit value accompanied by the unusual drop of the normalized water flux of film 4.5 (Table II). The reason for such a behavior is not quite clear yet, but it could be found in the varying role of formamide in CA dissolution process. When the formamide concentration in the solution exceeds a certain value, it might be assumed that formamide nonsolvent function predominates over its hydrogen-bonding action.

It is interesting to note that in solutions 2.6, 3.5, and 4.5, another effect appears, which manifests itself in the noticeable rise of their R_c values (Fig. 4). Taking into account the physical meaning of the R_c values, the latter effect might suggest the beginning of the phase inversion process, i.e., the incipient formation of the dispersed phase droplets within the CA network. Such a droplet nucleation in the metastable solution, as is well known, usually precedes the visual observation of the phase transition from the stable to the un-

stable two-phase system. The incipient droplets formation occurs earlier and is more easily observed in the case of solutions with a larger amount of formamide (a droplet-making agent). For this reason, the effect is more pronounced in solution 3.5 and particularly in solution 4.5.

CONCLUSIONS

Light-scattering measurements of the concentrated CA solutions have proved to be very useful for a detailed analysis of the porous asymmetric membrane formation mechanism. The results of anisotropic scattering are specially important, because they allow the assessment of the extent of supermolecular structurization in the membrane-casting solution.

A correlation of the anisotropic scattering results for various ternary (CA–acetone–formamide) casting solutions with those obtained by the asymmetric membrane testing has led to the improved concept of the membrane formation mechanism. A detailed description of the latter shows that the extent of the casting solution ordering, which can be modified by the variation of the solution composition, affects the porosity of the surface region of the eventually formed asymmetric membrane. The increase in the CA/F ratio of the casting solution increases the dimensions of the supermolecular network in it, and finally decreases the average membrane pore size. From both anisotropic and concentration scattering data as well as from the membrane properties, it can be concluded that formamide in the casting solution may have two different functions depending on its concentration. In a fairly wide range of lower concentrations, it decreases the size of supermolecular structures in the casting solution; at concentrations bringing the ternary casting solution close to the phase separation conditions, the formamide nonsolvent function predominates, causing the extensive ordering in the solution.

References

1. S. Loeb and S. Sourirajan, Dept. of Engineering, University of California, Los Angeles, Report No. 60-60, 1961.
2. R. E. Kesting and A. Menefee, *Kolloid-Z. Z. Polym.*, **230,** 341 (1969).
3. R. E. Kesting, *Synthetic Polymeric Membranes,* McGraw-Hill, New York, 1971, Chap. 5.
4. B. Kunst and S. Sourirajan, *J. Appl. Polym. Sci.*, **14,** 723 (1970).
5. B. Kunst and S. Sourirajan, *J. Appl. Polym. Sci.* **14,** 1983 (1970).
6. B. Kunst and S. Sourirajan, *J. Appl. Polym. Sci.*, **14,** 2559 (1970).
7. R. Pilon, B. Kunst, and S. Sourirajan, *J. Appl. Polym. Sci.*, **15,** 1317 (1971).
8. L. Pageau and S. Sourirajan, *J. Appl. Polym. Sci.*, **16,** 3185 (1972).
9. B. Kunst and B. Floreani, *Kolloid-Z. Z. Polym.*, **251,** 600 (1973).
10. B. Kunst and S. Sourirajan, *J. Appl. Polym. Sci.*, **18,** 3423 (1974).
11. R. Bloch, M. A. Frommer, O. Kedem, I. Feiner, A. Kedem, and D. Lancet, Research and Development Progress Report No. 499, Office of Saline Water, U.S. Department of the Interior, Washington, D.C., 1969.
12. M. A. Frommer, R. Matz, and U. Rosenthal, *Ind. Eng. Chem., Prod. Res. Develop.*, **10,** 193 (1971).
13. M. A. Frommer and D. Lancet, in *Reverse Osmosis Membrane Research,* H. K. Lonsdale and H. E. Podall, Eds., Plenum Press, New York, 1972, p. 85.
14. H. Strathmann, P. Scheible, and R. W. Baker, *J. Appl. Polym. Sci.*, **15,** 811 (1971).
15. H. Strathmann and P. Scheible, *Kolloid-Z. Z. Polym.*, **246,** 669 (1971).

16. M. T. So, F. R. Eirich, H. Strathmann, and R. W. Baker, *J. Appl. Polym. Sci., Polym. Lett. Ed.*, **11**, 201 (1973).

17. G. J. Gittens, P. A. Hitchcock, D. C. Sammon, and G. E. Wakley, *Desalination*, **8**, 369 (1970).

18. M. Panar, H. H. Hoehn, and R. R. Hebert, *Macromolecules*, **6**, 777 (1973).

19. N. Šegudović and Gj. Deželić, *Croat. Chem. Acta*, **45**, 385 (1973).

20. Gj. Deželić, *Pure Appl. Chem.*, **23**, 327 (1970).

21. O. G. Tarakanov, A. I. Demina, N. A. Abaturova, and I. N. Vlodavets, *Dokl. Akad. Nauk SSSR*, **180**, 164 (1968).

Received July 14, 1975